

Feasibility study for PET radioisotope production with plasma focus device

Abstract

Short-life radioisotopes (SLR) s such as 18F, 15O, 13N and 11B have been generated with a PF machine using 1-14 MeV (10^{12} per pulse) for 10B, 14N, and 16N. SLRs are simulated with GEANT4.10.7 and MCNPX codes. The elements are calculated to consist of flux, deposit, activity, rate of radioisotope produced, and radiation. In this paper, arguments are represented showing that a modest-sized PF machine using a 50 -75kJ fast capacitor bank when operated at pulse frequencies of 1-10Hz can produce SLRs/pulse. This paper reports the results of testing a PF as a generator of SLRs with dual applications for (i) secondary radioactive nuclear beams ion sources ($Z < 35$), and (ii) as a generator of radioisotopes for biomedicine ($Z < 10$) and/or PET imaging. The calculated sufficient thickness – energy for the proton (H^+) beam collision with SRIM 2011 code has been done. The results of the study aimed to evaluate the production of SLRs such as 11C, 13 N, and 15O. The obtained results with modified Iranian Sun Mather (IS) type DPF geometers are discussed and presented. This is a theoretical study. It is useful to use the results of this study for optimizing the device parameters for real experiences.

Keywords: Dense plasma focus, Short-lived radioisotope, Activity, MCNPX code, and Geant4 toolkit.

Hiva Rokhzadi-Zardouei¹, Mostafa Hasanzadeh*², Abdollah Refaei³ and Seyed mahmud Sadat-Kiai⁴

^{1,3}Department of Physics, Sanandaj Branch, Islamic Azad University, Sanandaj, Iran

²Reactor and Nuclear Safety Research School, Nuclear Science and Technology Research Institute (NSTRI), AEOL, Tehran, Iran

⁴Plasma and Nuclear Fusion Research School, Nuclear Science and Technology Research Institute (NSTRI), AEOL, Tehran, Iran

*Corresponding Author: Mostafa Hasanzadeh

Email:

m_hassanzadeh1354@yahoo.com

1. Introduction

Short-lived radioisotopes are positron (β^+) emitters and are now routinely produced by a baby cyclotron or a specially equipped reactor. They are mostly used in positron emission tomography (PET). Fluorine 18 (18F) is one of the most positron emitters used in medicine as flour deoxyglucose, an investigational drug being studied as an anticancer and antiviral agent radiotracer. It has a longer half-life compared to the others 109.771 minutes. Fluorine 18 decays by 97% positron emission (0.633 MeV) and an electron capture of 3%, (1.6555 MeV). With both modes of decay yielding a stable oxygen-18. The use of 18F for adults in Europe is about 4.7-9.5 mCi and in the USA is 10-20 mCi.

With the present technology, short-lived radioisotopes are easy to produce in a dense plasma focus (DPF). The arguments are that the device can produce cheaper SLRs because its primary capital and maintenance are much less than those machines mentioned above.

More, its operation is much easier and will take less working space as they must be produced in place due to the short lifetime. In general, we use highly energetic DPF, one has to use a low repetition rate for SLR production. inversely, if the device is excited with low bank energy, one must use a high repetition rate for SLR production.

There are four types of SLRs used in PET: 18F, 15O, 13N, and 11C. However, there are some new coming SLRs such as 62Cu. The production of SLRs in a DPF follows two processes; endogenous or thermonuclear process and exogenous which is a non-thermonuclear or beam-target process. In this work, the production of SLRs takes through the bombardment of the appropriate solid targets, therefore the beam-target process, by charged and uncharged particle beams. The solid targets made

of 10B, 12C, and 14N were placed 10 km far the top of the anode inside the IS DPF device to produce 11C, 13N, and 15O. The input particle energy for the program is taken as 1 MeV to 15 MeV with MCNPX code and Geant4 toolkit and finally, the results are compared.

2. Material and method

2.1. Dense plasma focus

The Plasma Focus (PF) was independently discovered by J. Mather [1] and N.V. Filippov [2] in the late '50s. Since then, many laboratories have studied the plasma-focus phenomenon and its remarkable capabilities for producing short pulses (1-300 ns) of X-rays, neutrons, and fast ions depending on the PF mode of operation. PF operation can be briefly described as a five-stage process (see Fig 1) with the appearance of high-energy ions and nuclear reactions occurring in the last stage. IS plasma focus is Mather one.

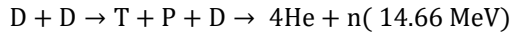
A dense plasma focus device, which is an electric discharge, is very suitable for studying the dynamics of the plasma and is a simple source for neutron, x-ray, and ion beams. The device includes an anode and a cathode, separated by a special insulator that causes a breakdown during the discharge of the capacitors. Such a device is usable for 0.5- 1 MJ facilities. There are two types of DPF, Filippov, and Mather. The vacuum chamber, turnover of spark-gap, and capacitor banks are the main components and the power supply, vacuum system, diagnostic tools, and automated data processing systems are the subdivisions part of the device. We have depicted in Fig. 1 a schematic of IS DPF.

Different gas fuels are used for various proposes at different pressures in a plasma focus device including helium, neon, argon, xenon, nitrogen, and deuterium. Neutron energy-distribution functions enabled the determination of axial and

radial components of energy of deuterons producing the fusion neutrons, as well as a rough evaluation of the total energy distribution of all fast deuterons in the pinch.

It was found that the total deuteron energy-distribution function decreases with the deuteron energy more slowly than the tail of the Maxwellian distribution for 1–2-keV deuterons.

Used deuterium (D) gas source in this study to generate the following reactions; $D + D \rightarrow 3He + n + 2.45 \text{ MeV}$



The high amount of deuteron energy distribution in DPF is $\leq 10 \text{ MeV}$,

Therefore, the maximum cross-sectional area of these reactions is within the range of deuteron energy defined in our target process. The DPF can be utilized as a multi-radiation source capable of simultaneously producing different types of radiation such as fusion neutrons ($\sim 2.45 \text{ MeV}$ from deuterium–deuterium (D–D) or 14.1 MeV from deuterium–tritium (D–T) fusion reactions.

Experimentally, this implies that if we have a clean vacuum chamber without or fewer impurities and for consecutive shots,

we can produce a considerable amount of $n14.1 \text{ MeV}$ and $P14.66 \text{ MeV}$ using D fuel. It is also possible to use a small amount of $3He$ as an admixture to enhance the reaction.

In addition, the process of compression in this device is performed in three stages: breakdown, plasma axial, and radial movements, and finally, pinch plasma.

After the plasma formation due to Lorentz force $F=J \times B$, the magnetic field begins to diffuse into the plasma column at the end of the final plasma compression phase, the magnetic field begins to diffuse into the plasma column. Moreover, the inductance of the plasma column strongly increases. This is due to the fast compression the rising voltage is in the form of a spike and a thin stream.

In a final form, the plasma focusing (pinch) is indicated in Fig. 1. All signals reach the oscilloscope with a delay of 3-5 ns, due to the signal transmission length .

In addition, we have displayed the physical constants with operational and geometrical parameters of the modified IS DPF in Table 1.

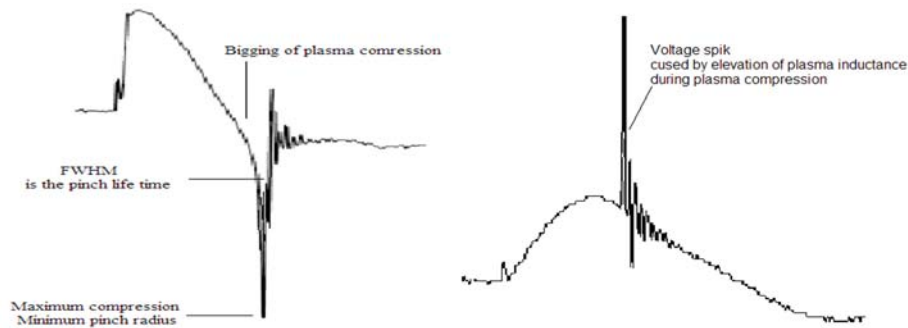


Fig. 1. Typical experimental signals vertical axis; (left) current derivative vertical

axis, (right) corresponding voltage horizontal axis.

The central electrode diameter is $\phi \approx 50 \text{ mm}$, and the chamber is filled with a gas mixture at $p = 0.1 \text{ e-}7 \text{ Torr}$ numbers refer to plasma development stages: I - the plasma sheath is formed, the plasma sheath moves toward the anode nozzle ($v \approx 10^5 \text{ m/s}$), the sheath arrives at the end of the anode and rearranges itself

into a cylinder with a conical opening, the plasma is compressed at the 10^{25} ions, the plasma column quickly develops instabilities associated with high-energy isotopes that can be utilized for the production of exotic and/or radioactive ion beams for radioactive ion beam applications and/or for medical imaging (PET) and biomedicine applications.

Table 1. The operational and geometrical parameters of IS DPF.

Specific heat ratio of the deuterium γ	$\frac{5}{3}$
Deutrium in mass m_d	$\times 10^{-27}$ kg
Trtium on mass m_t	10^{-2} kg
The density of deuterium ρ_d	$1.32 \times 10^{-3} \frac{\text{kg}}{\text{m}^3}$
The permittivity of free space ϵ_0	$8.854 \times 10^{-12} \left(\frac{\text{F}}{\text{m}}\right)$
Electric charge e	1.602×10^{-19} (C)
The pressure of D gas	10 torr
Impedance $Z_0 = \sqrt{\frac{L_0}{C_0}}$	$Z_0 = 12.5$ m Ω
Peak circuit current = $I_0 \approx \frac{V_0}{\sqrt{\frac{L_0}{C_0}}}$	$I_0 = 433445$ A
Maximum charging voltage V_0	$V_0 = 30$ kV
Capacitor bank C_0	$C_0 = 34$ μ F
Stored bank energy E	15 kJ
The inductance of the circuit L_0	160×10^{-9} H
Period of circuit trace T_0	$t_0 = 2\pi \sqrt{L_0 C_0} = 3.6$ μ s
Anode radius a	1.5 cm
Anode length Z_0	15 cm
Cathode radius b	5.25 cm
Axial speed V_a	$4.7 \times 10^4 \frac{\text{m}}{\text{s}}$
Radial speed V_r	$1.15 \times 10^5 \frac{\text{m}}{\text{s}}$
Pinch radius r_p	1.8 mm
Pinch life- time τ_p	30 ns
Pinch length d	1.2 cm
$c = \frac{b}{a}$	3.5
Current loss factor	0.6
Mass-sweep factor f_m	0.2
Induced voltage ϕ	8.1×10^4 V

Maximum compression corresponds to the thermonuclear reaction and if the fuel in Deuterium (D), formation of nuclear heat produces neutrons pinch formation. The radiation rate of these neutrons is obtained using the following equation;

$$R_{th} = \frac{1}{2} n^2 \sigma \bar{v}_{th} \quad (1)$$

Where n is the plasma density and $\sigma \bar{v}_{th}$ is the average cross-sectional area of the two colliding deuterons with each other and their velocity at thermal equilibrium.

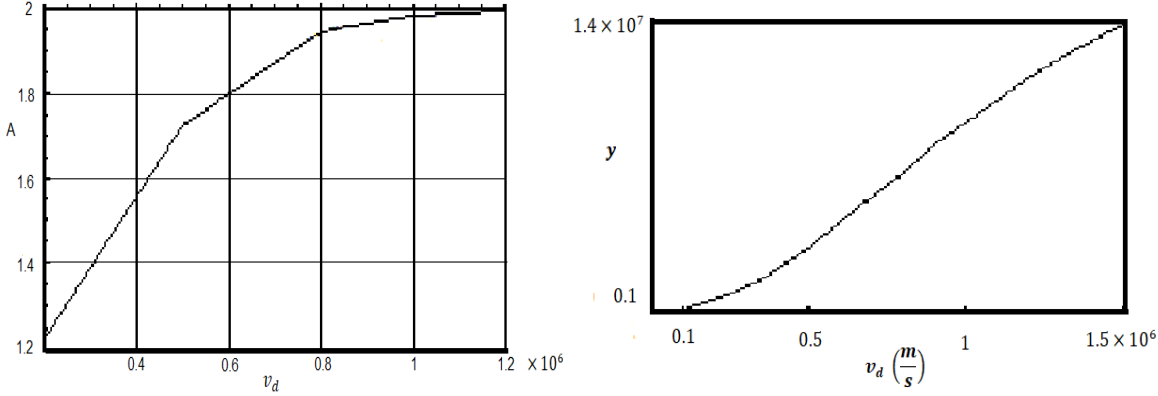


Fig. 2. vertical anisotropy axis (left) and the neutron yield vertical axis. (right) versus deuteron drift velocity

At this stage, the plasma column has exploded, with low plasma density and the mechanism that produces neutrons is non-thermonuclear or the beam target. In this case, the total nuclear rate reaction will be:

$$R_t = \frac{1}{2} n^2 \bar{\sigma} v_{th} + n n_a (\bar{\sigma} v_d - \bar{\sigma} v_{th}) \quad (2)$$

Where n_a is the medium density and v_d is the drift velocity.

Incidentally, the nuclear rate reactions in both mechanisms thermonuclear and non-thermonuclear are different. If we assume that thermonuclear reactions occur at thermal equilibrium then, the mechanism of the non-thermonuclear reaction is anisotropic [10];

$$A = \frac{1}{y} \left(1 + \frac{v_d}{v_0} \right) + 2 \left(1 + \frac{1}{y} \right) \left(1 + \frac{v_d}{v_0} \right) \quad (3)$$

Where:

$y = 1 + 2 \left(\frac{n_a V_a}{n V} \right) \left(\frac{\bar{\sigma} v_d}{\bar{\sigma} v_{th}} - 1 \right) n_a V_a$, is the density of the medium and V is the plasma volume. Although we work only with the beam-target process, adding the amount of $\bar{\sigma} v_{th}$ to Eq. 1 can be justified. This anisotropy and the neutron yield have been determined and the values found concerning the drift velocity are shown in Fig. 2. The production of SLRs in IS DPF uses an exogenous method, which is beam-target and non-thermonuclear mechanisms and benefits an anisotropy fact to complete the reactions.[1-3]

2.2. Theoretical method

Many experimentally and theoretical research works have been done using the beam-target mechanism to produce SLRs [4-7]. Experimentally the test of radioisotopes production in the pf-plasma radioactivity (decay curve) is measured by use of a

thin-wall, cylindrical Geiger-Muller counters (GM) having walls (cathode) made of high resistivity metal alloy (no Al or Cu). GM counters were used because they can survive an electromagnetic shock and jets of plasma emitted during PF operation. In the course of experiments, various geometrical set-ups were used Plasma origin of the radioisotopes breeding is supported by three observations; For PF discharges with a chamber Ta-clad and filled with a mixture of deuterium and one HZ component (12C, 14N and/or 16O) only one T1/2, as expected from (d, n) reaction product, is observed; no radioactivity occurs for pure D₂ fillings. Whenever the PF-chamber is filled with different relative compositions of HZ and LZ gases while keeping the total atomic density constant. In experiments with Al or Cu external targets and the chamber filled with HZ and LZ gases, two radioisotopes are produced: one in the plasma and one in the target.

Here, we use IS DPF device as an accelerator and simulated characteristics of effective conditions when using the device, with MCNPX code and GEANT4 toolkit for SLRs production. Eventually, the obtained results will be analyzed and compared. The detailed and extensive library of the cross-section in Monte Carlo MCNPX code software is used to simulate the geometry of the desired cells, source, etc. [8-9].

The calculated thickness – energy for the proton collision with SRIM 2011 code is shown in Fig.3. The energy of the particles is considered to be 5 to 15 MeV. The anode tip of IS DPF source is located 10 cm far from the target cubic. The geometrical target size consists of a solid cubic with 15×15 cm² and 7 mm thick. The targets are filled with 14N then by 10B and, 12C. Outside this cube, a sphere with a radius of 30 cm with air is placed as shown in Fig.5.

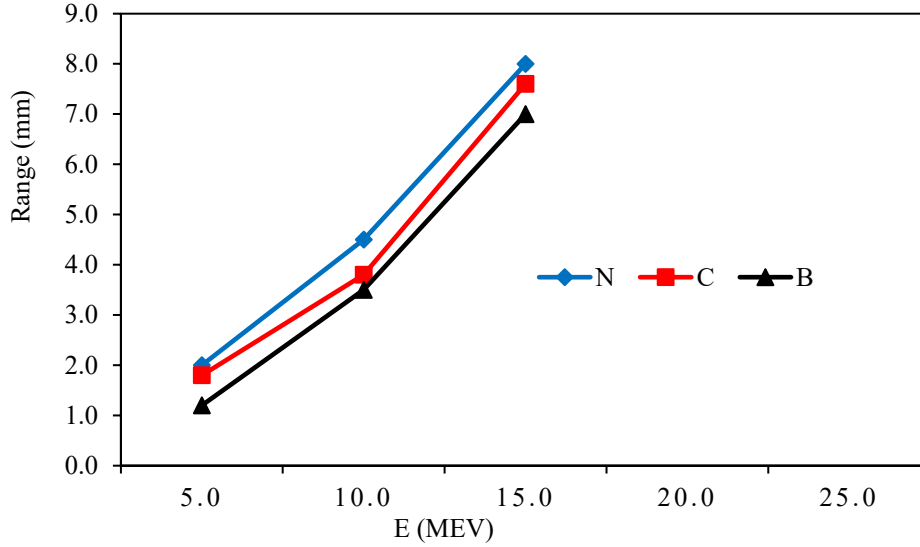


Fig. 3. Thickness range targets for the proton(H^+) collisions in term mm-MeV with SRIM 2011 code

In Fig. 5, we have depicted IS DPF geometry simulated by MCNPX code for this work. ENDF/B-IV library file uses the code calculate the parameters including current, flux, energy, and dose.

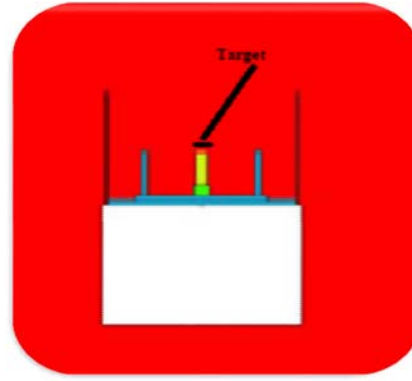
The deuteron, neutron, and proton fluxes are used to determine the activity of ^{11}C , ^{13}N , ^{15}O , and ^{18}F SLRs.

The advantage of the GEANT4 code compared to other simulation programmes is it is open-source, i.e. there is free

access to libraries; it can simulate the geometry of the software, and then import it into the software. In addition, the GEANT4 code has a DNA packet that can simulate chromosomal and dosimetry failure on a Micro Nanoscale. In Geant4, with the definition of CELLFLUX, we can calculate the neutron flux from D-D fusion for 1014 particles. GEANT4 is a free tool for simulating particle paths in the matter and is a reference simulation engine for LHC experiments at CERN and high-energy labs around the world [10-15]



(a)



(b)

Fig. 4. (a) IS DPF, (b) IS DPF geometry simulated for the SLRs production by MCNPX code

The neutron and proton fluxes ejected from the target are determined using Eq. (4).

$$F2 = \iiint_{A t E} \phi(\vec{r}, E, t) dE dt \frac{dA}{A} \quad (4)$$

Where, $\phi(\vec{r}, E, t)$ is surface output flux, A is the flux crossing surface, t is the time for the particle to pass through the surface, E is particle output energy, and r crossing surface coordinate [15-17].

The F2 Tally, which has the same role as the plate detector and gives the surface output flux, was used in the simulation. The results of the number of particles transported have been normalized and printed in the output. The F2 card in Eq. (4)

3. Results and discussion

The neutron flux emitted from cubic targets for the target elements is calculated with MCNPX code, as shown in Fig. 5(a). The results perform that by increasing the energy of neutrons, the flux of emitted neutrons approximately linearly increases. Nevertheless, the number of nucleons and larger cross-sectional create the maximum output flux in ^{14}N and its lowest value in the ^{10}B target, which has an especially high absorb cross-section. The total yield rate of the particles generated from the source of IS DPF is considered to be 1014 n/s . The results from these two codes showed that by increasing the energy of the neutrons in the targets which correspond to the gradient flux of neutrons, oscillating in low energy but about constant in high energies.

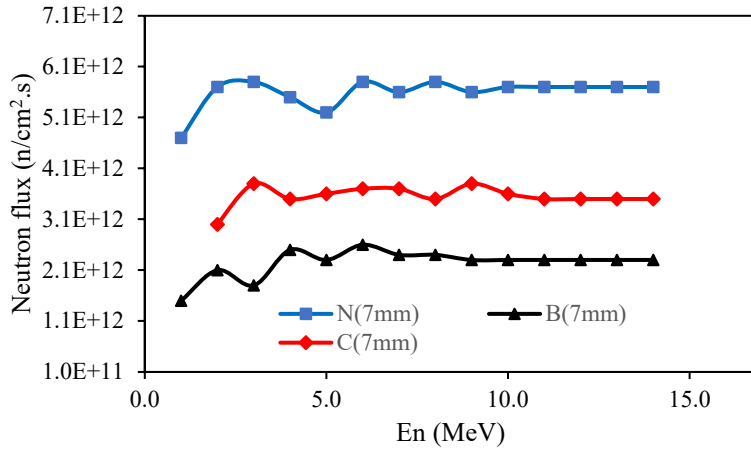


Fig. 5(a) The neutron flux emitted from the solid cubic targets filled with ^{14}N , ^{12}C , and ^{10}B for the neutron source in terms of energy with MCNPX code.

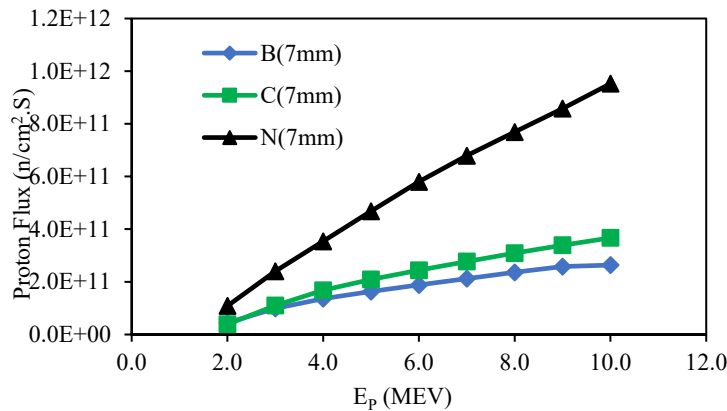


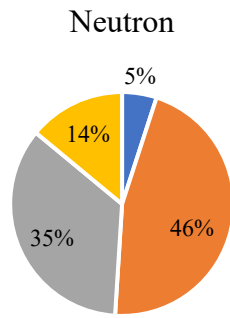
Fig. 5(b). The proton flux emitted from the solid cubic targets; ^{14}N , ^{12}C , and ^{10}B for the proton source in terms of energy with MCNPX code.

The same conditions of simulations, Fig.6. shows other particles produced by (a) neutron beams (b) proton beams, and (c) deuteron beams. collisions with a carbon target. Figure

The proton flux values within the solid cube targets, ^{14}N , ^{12}C , and ^{10}B for the proton source in terms of energy are shown in Fig. 5(b). The results show that by increasing the energy of protons, the flux of protons is increased linearly but, its maximum value is for the ^{14}N target and its lowest value for the ^{10}B target due to different cross-section interactions. As ^{14}N has a greater number of nucleons due to thinner thickness and Coulomb force, it faced less flux of protons.

The protons may be leaving due to billiards nuclei collision. It should be noted that in all the calculations, the error value of the programs was less than $0.001(\text{n/cm}^2\cdot\text{s})$.

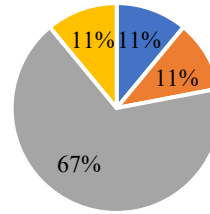
10(c) shows the result of deuteron beams collisions to produce ^{15}O (20%) and ^{13}N (2%). Finally, the results show that the deuteron beam collisions had the best results for producing the wanted medical radioisotopes for the carbon target within the plasma focus device. [22]



■ O16 ■ N14 ■ C13 ■ B10

(a)

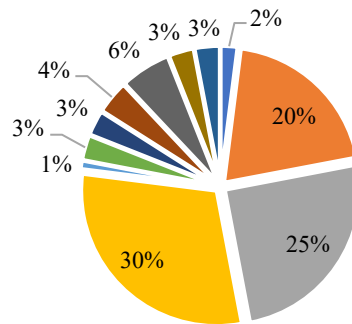
Proton(H⁺)



■ O16 ■ O14 ■ N14 ■ C13

(b)

Deuteron



■ O17 ■ O15 ■ N15 ■ N14 ■ N13 ■ He3 ■ F17 ■ C13 ■ C12 ■ C11 ■ B11

(c)

Fig.6 showed radioisotopes produced in carbon targets with, neutron beams (a), proton beams (b), and deuteron beams (c) with the Geant4 toolkit.

4. Conclusion

This paper presents a simulation by MCNPX code and Geant4 toolkit using neutron, proton, and deuteron sources for producing of SLRs within an IS DPF device. The approach relies on a fast pulse of particles produced by IS DPF device as a breeder. The energy spectrum is not strictly mono-energetic but contains various energies as in the high-energy of the proton and deuteron distributions. In addition, the production of 14.1MeV neutron by Deuterium that resulted in the second D- T reaction as a flux of nuclear fusion is interesting. The results showed: that by increasing the neutron energy and the neutron fluxes increased, it would be promising to scale up the approach to the optimum achievement of 1 MBq activity. Deuteron beams collisions have the best yield for producing 15O and 13N with carbon targets.

Acknowledgments:Non

Conflict of Interests: Non

Ethical Considerations: Non

Financial Disclosure: Non

Funding/Support: Non

References

- [1] S. GB., Radioactive decay and interaction of radiation with matter, basics of pet imaging. Cham: Springer; 2016.
- [2] EL. Cole, MN. Stewart, R. Littich, et al. Radio syntheses using fluorine-18: the art and science of late-stage fluorination. *Curr Top Med Chem* 2014; 14(7):875–900.
DOI: [10.2174/1568026614666140202205035](https://doi.org/10.2174/1568026614666140202205035)
- [3] F. Castillo et al. Evidence of Thermal and Non-Thermal Mechanisms Coexisting in Dense Plasma Focus D-D Nuclear Reactions *J. Phys. D: Appl. Phys.* 33 (2000) 141-147.
DOI: [10.1088/0022-3727/33/2/308](https://doi.org/10.1088/0022-3727/33/2/308)
- [4] Mohamad mohamadzadeh, hosein ghiasi, skyng dose estimations for an 18 Mev photon Beam Using MCNPX cod: A comparison of flattened and flattening filter- free beam, *Frontiers in Biomedical Technologies*, Vol. 8, No. 3 (2021) 219-225
- [5] P. Kubas, et al. Determination of Deuteron Energy Distribution from Neutron Diagnostics in a Plasma-Focus Device, *IEEE TRANSACTIONS ON PLASMA SCIENCE*, VOL. 37, NO. 1, JANUARY 2009 .
DOI: [10.1109/TPS.2008.2005899](https://doi.org/10.1109/TPS.2008.2005899)

- [6] S. H. SAW, et al. Scaling Laws for Plasma Focus Machines from Numerical Experiments, *EPE* Vol.2 No. 1, February 2010. DOI: [10.4236/epe.2010.21010](https://doi.org/10.4236/epe.2010.21010)
- [7] A. E. Abdou, et al. Preliminary Results of Kansas State University Dense Plasma Focus, *IEEE TRANSACTIONS ON PLASMA SCIENCE*, VOL. 40, NO. 10, OCTOBER 2012
- [8] M. mu'alim et al. Monte Carlo N Particle Extended (MCNPX) Radiation Shield Modelling on Boron Neutron Capture Therapy Facility Using D-D Neutron Generator 2.4 MeV, *Indonesian Journal of Physics and Nuclear Application*, Vol. 4, No. 2, June 2019
- [9] Tekin HO, Singh VP, Altunsoy EE, Manici T, Sayyed M. Mass Attenuation Coefficients of Human Body Organs using MCNPX Monte Carlo Code. *Iran J Med Phys* 2017; 14: 229-240. DOI: [10.22038/ijmp.2017.23478.1230](https://doi.org/10.22038/ijmp.2017.23478.1230).
- [10] E boustani et al. Control rods reactivity worth calculation using deterministic and Monte Carlo approaches for an MTR type research reactor, *Iranian Journal of Physics Research*, Vol. 21, No. 3, 2021
- [11] S.M.Sadat Kiai, design a 10KJ is mather type Plasma Focus for solid target activation to produce short-lived Radioisotopes $^{12}\text{C}(\text{d,n})^{13}\text{N}$, *Fusion Energy*. Volume29, (2010), 421-426
- [12] A.Talaei et al, Interaction of the high energy deuterons with the graphite target in the plasma focus devices based on lee model, *Appl. Rad. Isotopes*, volume 68,(2010) 2218-2222
- [13] M. Nanbedeh, et al., A feasibility study of the Iranian Sun mather type plasma focus source for neutron capture therapy using MCNPX2. 6, Geant4 and FLUKA codes, *Nuclear Engineering and Technology*, Volume 25, (2019).
- [14] M.AKel, et al., Interaction of the high energy deuterons with the graphite target in the plasma focus devices based on Lee model, *Phys. Physics of Plasmas*, Volume 21, (2014), 072507-1.
- [15] S.Lee and S.H.Saw, Plasma focus ion beam fluence and flux—Scaling with stored energy, *volume (19)*, (2012), 112703 (1-5). DOI: [10.1063/1.4766744](https://doi.org/10.1063/1.4766744)
- [16] [Pejman Rowshanfarzad](#), [Mahsheed Sabet](#), [Amirreza Jalilian](#), and [Mohsen Kamalidehghan](#). An overview of copper radionuclides and production of Cu-61 by proton irradiation of Zn-nat at a medical cyclotron, *Vol 64(12)*, 2007, 1563-73. DOI: [10.1016/j.apradiso.2005.11.012](https://doi.org/10.1016/j.apradiso.2005.11.012).
- [17] *Physics Reference Manual* Version: geant4 10.1 (5 December 2014).